THE JOURNAL OF PHYSICAL CHEMISTRY C

ARTICLE

pubs.acs.org/JPCC

Functionalized Graphene Oxide Nanocomposite Membrane for Low Humidity and High Temperature Proton Exchange Membrane Fuel Cells

Hadis Zarrin,[†] Drew Higgins,[†] Yu Jun,[†,‡] Zhongwei Chen,[*,†] and Michael Fowler[†]

[†]Department of Chemical Engineering, Waterloo Institute of Nanotechnology, Waterloo Institute for Sustainable Energy, University of Waterloo, Waterloo, Ontario, Canada N2L 3G1

[‡]State Key Laboratory of Advanced Technology for Materials Synthesis & Processing, Wuhan University of Technology, Wuhan, Hubei, China 430070

ABSTRACT: Functionalized graphene oxide Nafion nanocomposites (F-GO/Nafion) are presented as a potential proton exchange membrane (PEM) replacement for high temperature PEM fuel cell applications. The GO nanosheets were produced from natural graphite flakes by the modified Hummer's method and then functionalized by using 3-mercaptopropyl trimethoxysilane (MPTMS) as the sulfonic acid functional group precursor. F-GO/Nafion composite membranes were fabricated by a simplistic solution casting method. Several physicochemical characterization techniques were applied to provide insight into the specific structure and morphology, functional groups, water uptake, and ionic conductivities of the membranes. Proton conductivity and single cell test results demonstrated significant improvements for F-GO/Nafion membranes (4 times) over recast Nafion at 120 °C with 25% humidity.

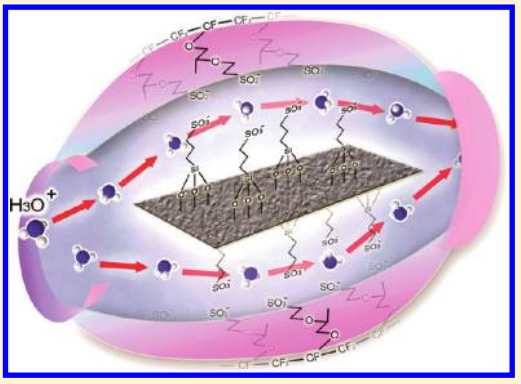

1. INTRODUCTION

Proton exchange membrane fuel cells (PEMFCs) are being developed intensively due to their great potential as environmentally benign energy conversion devices for transportation, residential, and portable applications.[1] Operation of PEMFCs at high temperatures (above 100 °C) would significantly boost their performance by enhancing the electrode reaction kinetics, limiting the excessive precious metal (Pt) catalyst requirement, along with improving the electrocatalyst CO tolerance and allowing easier thermal and water management of the system.[2] However, high temperature operation of PEMFCs is not practical while using the state-of-the-art hydrated perfluorosulfonic acid membranes (PFSA, under the commercial name of Dupont Nafion), as they require strict humidification under temperatures above 80 °C due to the evaporation of water from the membrane structure.[3−7] Considerable research efforts have been devoted to developing organic−inorganic composite membranes able to operate at increased temperatures. Incorporation of hygroscopic inorganic nanomaterials,[8−14] such as ZrO_2, SiO_2, TiO_2, P_2O_5, and Zeolite nanoparticles and TiO_2 nanotubes and nanowires, into the structure of the PFSA has been demonstrated to result in composite membranes with promising proton conductivity at high temperature and low relative humidity.[15−22]

Graphene oxide (GO) has been considered attractive for many applications owing to its unique thermal and mechanical properties.[23−25] Upon incorporation in PFSA, the unique structure and high surface area of the GO may provide more proton transport channels and hold more water, which could be beneficial for the improvement of the proton conductivity and mechanical properties of the membranes.[25−27] In the present work, the effects of functionalized graphene oxide (F-GO) nanosheets have been investigated as inorganic fillers in a Nafion composite membrane, fabricated by a simplistic solution casting method. The surface morphology, thermal stability, ion exchange capacity, water uptake, and proton conductivity have been investigated. Moreover, the performance of this composite membrane has been investigated in high temperature PEMFCs at low relative humidity conditions and found to provide good performance, rendering this material as a very promising material for application in PEMFCs operating at elevated temperatures.

2. EXPERIMENTAL METHODS

2.1. Synthesis of Graphene Oxide (GO). The graphene oxide (GO) nanosheets were produced from natural graphite flakes by the modified Hummer's method.[25,28−30] Graphite powder (2 g) and sodium nitrate ($NaNO_3$, 1 g) were combined in a round-bottom flask. Concentrated sulfuric acid (H_2SO_4, 46 mL) was added while stirring in an ice bath at 0 °C. Potassium permanganate ($KMnO_4$, 6 g) was added very slowly because it is a strong oxidizing agent. The flask was removed from the ice bath and stirred for 1 h at room temperature. Distilled deionized water (DDI, 92 mL) was then added drop by drop, generating a significant amount of heat and gas. After further stirring for

Received: May 17, 2011
Revised: September 8, 2011
Published: September 14, 2011

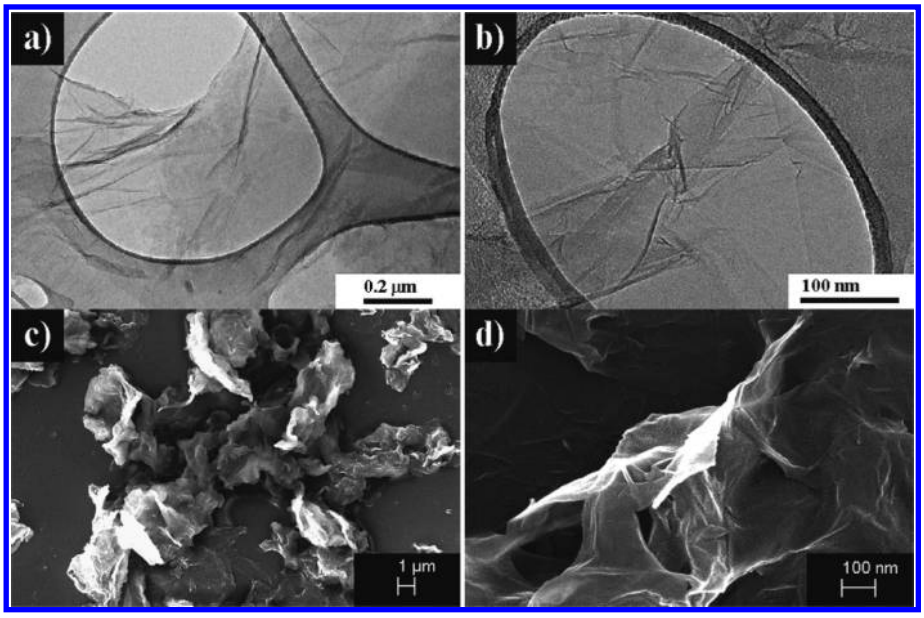

Figure 1. TEM of unmodified GO at (a) low magnification and (b) high magnification. SEM images of GO at (c) low magnification and (d) high magnification.

30 min, the reaction mixture was diluted with warm DDI water (280 mL), and 30% hydrogen peroxide (H_2O_2, 40 mL) was added to neutralize any remaining permanganate. The product was then filtered and washed with copious amounts of 5% hydrochloric acid (HCl), after which it was centrifuged several times until the excess HCl was removed, collected by filtration, and dried in an oven at 70 °C overnight.

2.2. Functionalization of Graphene Oxide (F-GO) with Sulfonic Acid-Containing Groups. The functionalization of GO (F-GO) nanosheets was performed by using 3-mercaptopropyl trimethoxysilane (MPTMS) as the sulfonic acid functional group precursor.[31] The reaction was carried out in toluene at a temperature of 110 °C under reflux conditions for 24 h, with 1:15:70 weight ratios of GO, MPTMS, and toluene, respectively. The mercapto groups grafted onto the GO nanosheets were then oxidized to sulfonic acid groups by using 30 wt % H_2O_2 solution at 25 °C for 24 h. The prepared samples were filtered and washed with ethanol and water to remove the precursor residue. Samples were dried overnight prior to characterization.

2.3. Casting F-GO/Nafion Nanocompposite Membrane. F-GO/Nafion composite membranes (5 or 10 wt %) were casted by mixing 5 or 10 wt % F-GO with an appropriate amount of Nafion 1100 EW solution (5%, DuPont) and ethanol. Then, the mixtures were ultrasonicated for 30 min and heated at 60 °C until half of the solution evaporated. Finally, the mixture was heated at 100 °C for 2 h and then 140 °C for 1 h.[32] Both pure Nafion and F-GO/Nafion composite membranes were pretreated by boiling in a 3% H_2O_2 aqueous solution for 1 h, rinsed in boiling deionized water for 1 h, boiled in 0.5 M H_2SO_4 for 1 h, and finally rinsed again in deionized water before being tested.[33]

2.4. Proton Conductivity Measurement. The proton conductivity of GO and F-GO powders was estimated by using a two-electrode setup.[35] First, each of the powdered samples was individually loaded into a tube cell with a diameter of 1.6 mm in which the two electrodes are inserted from the top and bottom. Then, they were pressed for several hours. To attain water-saturated conditions, the fixture was disassembled from the top, and 20 μL of double deionized water was injected with a syringe onto the sample in each cell. The water was allowed to soak into the samples for 30 min. The top electrodes were then replaced; the fixture was reassembled; and the sample cells were retorqued. The proton conductivity was measured at 100% relative humidity at different temperatures ranging from 20 to 80 °C to probe the effect of sulfonic acid functionalization on the GO ionic conductivity.

The proton conductivity of all membranes was obtained by a four-electrode method using AC impedance spectroscopy[36] with potentiostat control (CHI760D model). The impedance was measured in the frequency range between 1 MHz and 0.1 Hz with a perturbation voltage amplitude of 5 mV. The humidity was controlled by mixing water-saturated nitrogen gas with dry nitrogen gas, while the system temperature was fixed at 80, 100, and 120 °C. This method effectively avoids contact resistance, and the results are very reproducible. The proton conductivity (σ) of all powdered samples and membranes was then determined along the longitudinal direction, using the following equation[37−39]

$$\sigma = \frac{L}{AR} \tag{1}$$

where σ, L, R, and A denote the ionic conductivity, sample length (or distance between the reference electrodes in the membrane), the resistance of the powder/membrane, and the cross-sectional area of the powder/membrane, respectively.

2.5. Water Uptake (WU) and Ion Exchange Capacity (IEC). To measure the water retention capability of the membranes, the WU (%) was calculated. For this, the membranes were first immersed and saturated in deionized water at room temperature for 24 h. They were then taken out and weighed immediately after the water droplets were removed from the surface. Following this, they were vacuum-dried at 80 °C for 24 h, put into a plastic sealing bag immediately, and weighed. The WU was determined from the following equation[40,41]

$$\mathrm{WU}\ (\%) = \frac{W_{\mathrm{wet}} - W_{\mathrm{dry}}}{W_{\mathrm{dry}}} \times 100 \tag{2}$$

dx.doi.org/10.1021/jp204610j |J. Phys. Chem. C 2011, 115, 20774–20781

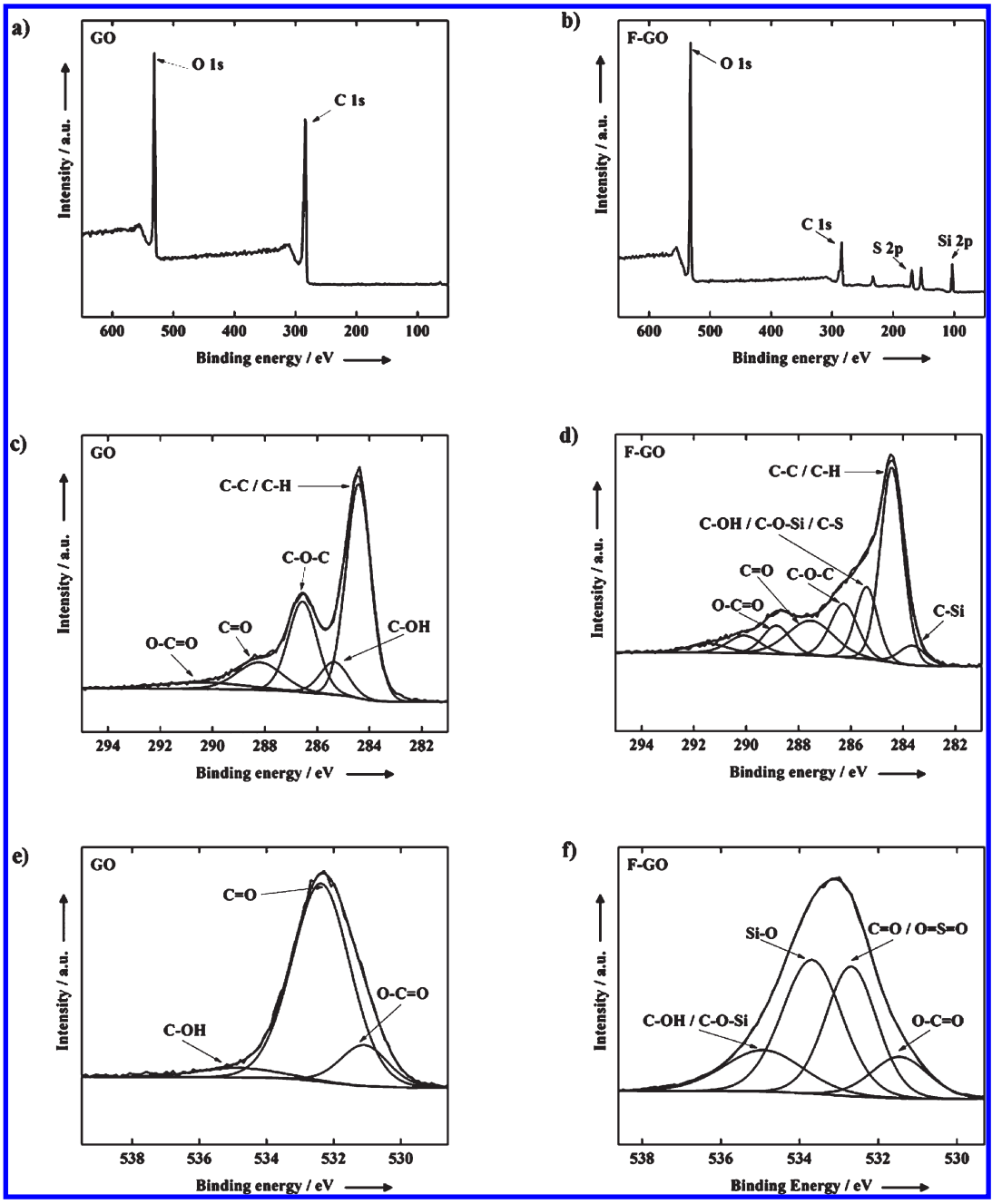

Figure 2. Wide region XPS spectra of (a) GO and (b) F-GO. Deconvoluted XPS spectra in the C1s region for (c) GO and (d) F-GO. Deconvoluted XPS spectra in the O1s region for (e) GO and (f) F-GO.

where WU (%), W_{wet}, and W_{dry} are the water uptake by weight percentage, the weight of the wet membrane, and the weight of the dry membrane, respectively.

IEC of each membrane was determined by a back-titration method. At first, the samples were dried until the weight was constant, after which each sample was soaked in 0.2 M NaCl (50 mL) for 24 h to exchange sodium ions with protons in the composite membranes. Back titration was then accomplished with 0.01 M NaOH standardized solution, and IEC values were calculated by the following equation[42]

$$\mathrm{IEC} = \frac{V_{\mathrm{NaOH}} - C_{\mathrm{NaOH}}}{W_{\mathrm{dry}}} \quad (3)$$

where IEC is the ion exchange capacity (meq g^{-1}); V_{NaOH} is the added titrant volume at the equivalent point (mL); C_{NaOH} is the molar concentration of the titrant; and W_{dry} is the dry mass of the sample (g).

2.6. Physico-Chemical Characterization. The overall morphology of all samples was examined by using transmission electron microscopy (TEM, JEM-100CX II) and scanning electron microscopy (SEM, LEO FESEM 1530). X-ray photoelectron spectroscopy (XPS, Thermal Scientific K-Alpha XPS spectrometer) was used to investigate the surface elemental composition and atomic configurations of both GO and F-GO. Fourier transform infrared spectroscopy (FTIR, PerkinElmer-283B FT-IR Spectrometer) was used for determination of the

Table 1. Summary of C 1s and O 1s XPS Spectral Data

	sample	binding energy [eV]	assignment
C 1s	GO	284.4	sp^2 and sp^3 hybridized C−C/ C−H
		285.4	C−OH
		286.6	C−O−C
		288.2	C═O
		290.0	O−C═O
	F-GO	283.7	C−Si
		284.4	sp^2 and sp^3 hybridized C−C/ C−H
		285.4	C−OH/ C−O−Si/ C−S
		286.3	C−O−C
		287.6	C═O
		288.8	O−C═O
		290.1	$\pi-\pi^*$ shake up satellite of the sp^2 hybridized C
		291.5	$\pi-\pi^*$ shake up satellite of the sp^2-hybridized C
O 1s	GO	531.0	O−C═O
		532.4	C═O
		534.9	C−OH
	F-GO	531.5	O−C═O
		532.7	C═O/O═S═O
		533.7	Si−O
		534.9	C−OH/ C−O−Si

Table 2. Atomic Percentages of Pristine Graphene Oxide (GO) and Sulfonic Acid Functionalized Graphene Oxide (F-GO) Determined from XPS

sample	C [atom %]	O [atom %]	Si [atom %]	S [atom %]
GO	73.16	26.84	-	-
F-GO	36.03	44.76	3.73	15.48

functional groups present in the Nafion and F-GO/Nafion membranes.

2.7. Membrane Electrode Assembly (MEA) Fabrication and Testing. The performance of the 10 wt % F-GO/Nafion and recast Nafion membranes in a fuel cell setup was determined using a single-cell MEA setup fabricated using a decal method as described elsewhere.[34] The electrocatalyst used in the anode and cathode was Pt/C (20 wt %, E-TEK). Briefly, catalyst ink was prepared by mixing the catalyst with 5% Nafion solution for 1 h. Glycerol was subsequently added, and the solution was stirred for 24 h. After preparation, the catalyst ink was painted onto decal Teflon blanks and dried in an oven. This process was repeated until the desired catalyst loading was achieved. Each membrane sample was cleaned and boiled in a dilute NaOH solution to ion exchange the membrane to Na^+. After rinsing, the membrane was dried by hot pressing and then cooled prior to MEA fabrication. The MEA with an active electrode area of 5 cm^2 was obtained by pressing the cathode and anode onto each side of the recast Nafion or 10 wt % F-GO/Nafion composite membrane at 210 °C and 110 lbs cm^{-2} for 5 min. Decals could then be removed, leaving the catalyst layers firmly attached to the membrane surface. The MEA was assembled into the fuel cell hardware for testing. Catalyst loading was 0.2 mg_{Pt} cm^{-2} for the cathode and 0.1 mg_{Pt} cm^{-2} for the anode, and gas flow rates of 0.2 and 0.5 L min^{-1} were used for hydrogen and oxygen, respectively.

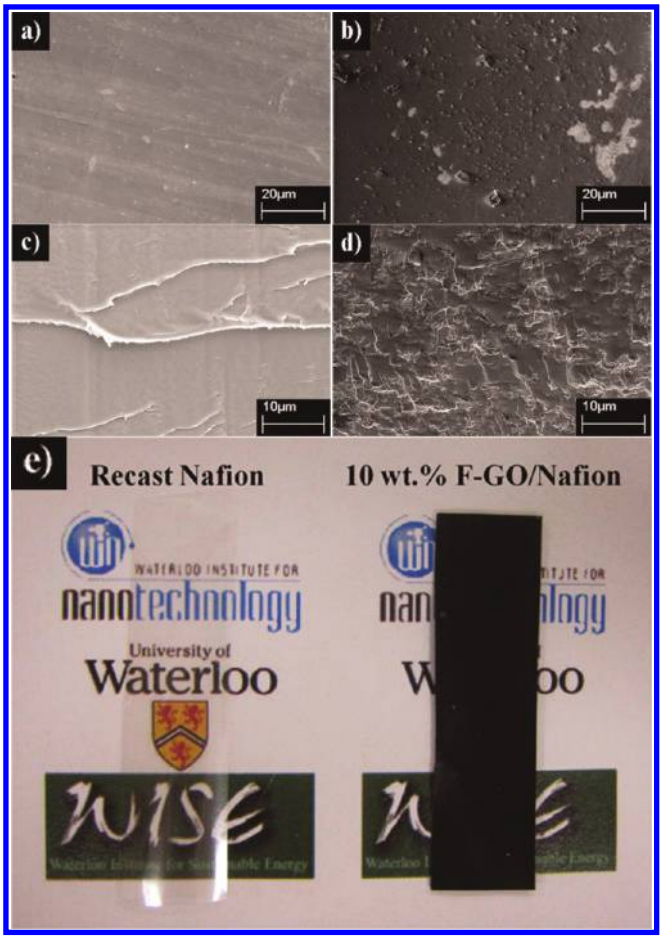

Figure 3. Top view SEM images of (a) recast Nafion and (b) 10 wt % F-GO/Nafion composite membrane. Cross section view of SEM images for (c) recast Nafion and (d) 10 wt % F-GO/Nafion composite membrane. (e) The pictures of recast Nafion and 10 wt % F-GO/Nafion composite membranes.

3. RESULTS AND DISCUSSION

The nanosheet structure and morphology of GO were investigated by TEM and SEM imaging as displayed in Figure 1. TEM analysis (Figure 1a,b) showed that the pristine graphene oxide nanosheets appeared relatively flat with some wrinkles, consistent with the morphology typically reported in the literature.[22,43−46] The SEM images of GO (Figure 1c,d) displayed the exfoliated layered structure of graphene oxide agglomerates.[9]

The chemical composition of both unmodified and functionalized GO was determined by XPS. Upon analysis of the wide-range XPS patterns displayed in Figure 2a,b, two new peaks were observed for F-GO at binding energies of 169.48 and 104.28 eV, attributed to S 2p and Si 2p components, respectively. This confirms the successful attachment of the sulfonic acid containing precursor (MPTMS) onto the surface of the GO nanosheets. Furthermore, upon high resolution analysis, no S 2p peak at a binding energy of 164 eV (corresponding to −SH) was observed, confirming the complete oxidation of −SH to $-SO_3H$ functional groups.[20] To provide more insight regarding the surface-decorated functional groups, deconvulated XPS spectra of the C 1s

dx.doi.org/10.1021/jp204610j |J. Phys. Chem. C 2011, 115, 20774–20781

(Figure 2c,d) and O 1s (Figure 2e,f) signals are provided for both GO and F-GO. Comparison of the C 1s signal clearly indicates a change in the degree of surface oxidation before (Figure 2c) and after (Figure 2d) MPTMS functionalization. F-GO (Figure 2d) demonstrates three new peaks (283.7, 290, and 291.5 eV; Table 1) other than those assigned to the GO surface functional groups. Moreover, the peak intensities and binding energies observed for F-GO are slightly different than those in GO. This is because of the exposure of highly reactive hydroxyl and epoxy groups[47−49] to the sulfonic acid containing precursor (MPTMS), leading to a decrease in the epoxy and hydroxyl components present on the surface, and the addition of new C−O−Si and/or C−S bonds contributing to the peak observed at 285.4 eV.

The functionalized graphene oxide has shown a greater concentration of surface oxygen, 44.76 atom %, compared to pristine graphene oxide, 26.84% (Table 2). The O 1s XPS peaks of GO in Figure 2e are composed of three components including O−C═O, C═O, and C−OH with their binding energy at 531.0, 532.4, and 534.9 eV, respectively.[44,49] These peaks are shifted to 531.5, 532.7, and 534.9 eV in F-GO with a new peak appearing at 533.7 eV, indicating the creation of Si−O bonds due to the addition of a sulfonic acid containing precursor, MPTMS (Figure 2f).

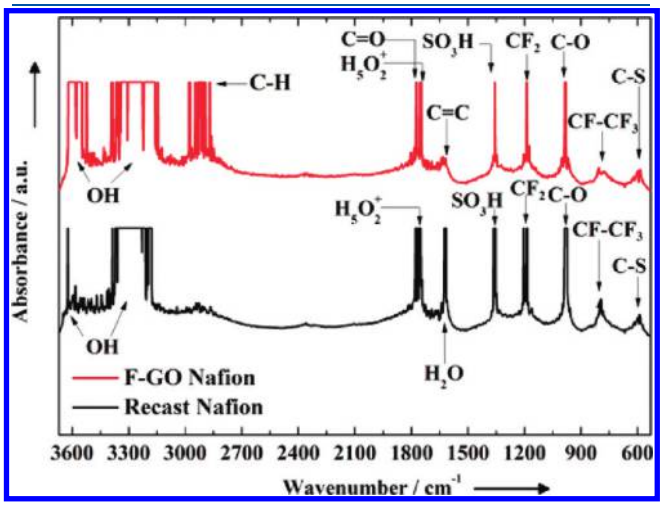

Figure 4. FT-IR spectra comparison between recast Nafion and 10 wt % F-GO/Nafion composite membranes.

Furthermore, the peak at 532.7 eV for F-GO has become more intense and shifted to slightly higher binding energies compared with that of GO (532.4 eV), assigned to a combination of C═O and O═S═O bonds, confirming the complete oxidation of −SH to $-SO_3H$.[20,50]

The top view SEM images of recast Nafion and 10 wt % F-GO/Nafion composite membranes were compared in Figure 3a and 3b to determine the changes of the Nafion membrane surface after grafting F-GO nanofillers. It was observed that the bare recast Nafion has a smooth surface, while after the incorporation of F-GO nanosheets the surface became significantly rougher. Also, it was seen that the surface of Nafion was uniformly covered with dark sheets of F-GO, indicating the successful grafting of sulfonated GO sheets onto the F-GO/Nafion electrolyte polymer surface. Cross-section SEM images of recast Nafion and 10 wt % F-GO/Nafion nanocomposite membranes are shown in Figure 3c and 3d, respectively. Distinct differences are observed, with the recast Nafion membrane presenting a relatively smooth cross section, whereas the F-GO/Nafion nanocomposite membrane displayed a very rough cross section. This is in agreement with the previous report by Lian et al.[51] Figure 3e provides visual comparison of the 10 wt % F-GO/Nafion nanocomposite membrane to the transparent recast Nafion.

For elemental analysis of the membranes, the Fourier-transformed infrared (FT-IR) spectrum of F-GO/Nafion was compared to that of recast Nafion (Figure 4). The assignments of the recast Nafion FT-IR spectrum was made by comparison with Nafion values obtained in the literature presented in Table 3.[52−56] The bands at 590, 793, 974, 1188, and 1354 cm^{-1} are typical of C−S, CF−CF_3, C−O, CF_2, and SO_3H groups which are in good agreement with previous reports.[57,58] The two bending frequencies of 1626 and 1760 cm^{-1} could be possibly assigned to H_2O and $H_5O_2^+$ species[53,59] since before FT-IR spectroscopy the membranes had not been completely dried and had low values of water content. The H-bonded OH stretching vibrations were in an extremely broad band region between 3178 and 3387 cm^{-1}, and the free sharp OH group band appeared at 3622 cm^{-1}.

In the F-GO/Nafion composite membrane, all of the expected functional groups of the Nafion backbone structure are observed (Figure 4, Table 3). The absence of peaks at 1060, 1250, and 1365 cm^{-1} indicates that all epoxide and hydroxyl groups attached to the basal pristine graphene layer have been removed,[52] confirming that they have been attacked and sulfonated by MPTMS. However, CF−CF_3 and C−O functional

Table 3. FT-IR Data Analysis for Recast Nafion and 10 wt % F-GO/Nafion Membranes

recast Nafion		10 wt % F-GO/Nafion	
wavenumber [cm^{-1}]	assignment	wavenumber [cm^{-1}]	assignment
590	C−S	590	C−S
793	C F−CF_3	801	C F−CF_3
974	C−O	982	C−O
1188	CF_2	1188	CF_2
1354	SO_3H	1354	SO_3H
1626	H_2O	1620	C═C
1760	$H_5O_2^+$	1748	C═O/$H_5O_2^+$
3178−3387	H-bonded OH	2893−3000	aliphatic $(CH_2)_3$
3622	free OH	3144	aromatic C−H
		3160−3368	H-bonded and carboxy OH
		3522−3620	free OH

dx.doi.org/10.1021/jp204610j |J. Phys. Chem. C 2011, 115, 20774–20781

groups are shifted to higher wave numbers of 801 and 982 cm^{-1}, respectively. This peak shift can be attributed to changes of the chemical surroundings which may also affect the extinction coefficient of different functional groups.[60,61] The absorption bands at 1620 and 1748 cm^{-1} confirm the existence of aromatic C═C and carboxy C═O/$H_5O_2^+$, respectively. The presence of aliphatic C−H is indicated by the band stretching from 2893 to 3000 cm^{-1}, assigned to the $(CH_2)_3$ chains in the MPTMS sulfonic acid precursor.[62] Adjacent to this region, a peak at 3144 cm^{-1} was observed which refers to aromatic C−H stretching vibrations. In the F-GO/Nafion membrane, the broad band of OH groups in the region between 3160 and 3368 cm^{-1} indicated the presence of both H-bonded and carboxy OH groups. Another broad band was also seen in the region between 3522 and 3620 cm^{-1} which is believed to be related to free OH groups.

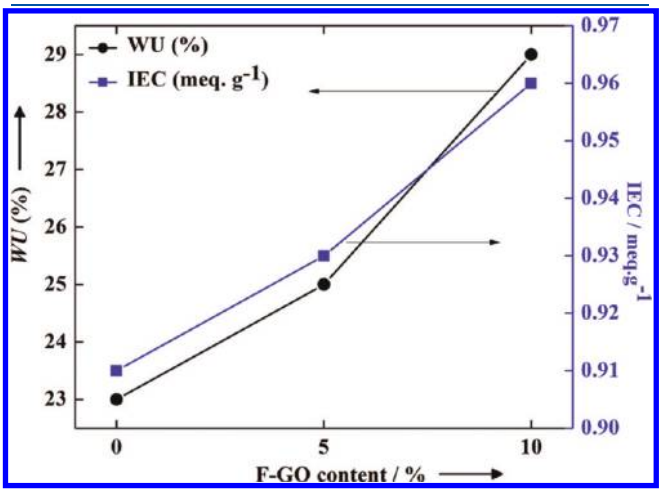

Figure 5. WU (%) and IEC (meq g^{-1}) of recast and composite Nafion membranes.

The water uptake (WU) and ion exchange capacity (IEC) of 5% and 10% F-GO/Nafion nanocomposite membranes are compared to that of recast Nafion as displayed in Figure 5. It is seen that the WUs of the F-GO/Nafion membranes are higher than that of recast Nafion, displaying WU values 2% and 6% higher for 5% F-GO/Nafion and 10% F-GO/Nafion, respectively. Furthermore, the IEC of the membranes was found to increase with higher F-GO contents such that 0.96, 0.93, and 0.91 meq g^{-1} were determined for 10% F-GO/Nafion, 5% F-GO/Nafion, and recast Nafion, respectively.

Figure 6a provides a comparison of the GO and F-GO powder ionic conductivity. The ionic conductivity of F-GO was found to be about 3 orders of magnitude higher at 20 °C and more than 1 order of magnitude higher at 80 °C than GO. This can be attributed to the higher sulfonic acid content of GO which helps the absorption and retention of more water, distinctively at high temperatures. In Figure 6b−d, the relative humidity dependence of the proton conductivity of the recast Nafion and the F-GO/Nafion composite membranes with 5 and 10 wt % loadings of F-GO are determined at temperatures of 80, 100, and 120 °C, using a four-electrode AC impedance method.[38,39] It can be observed that the incorporation of functionalized GO into the

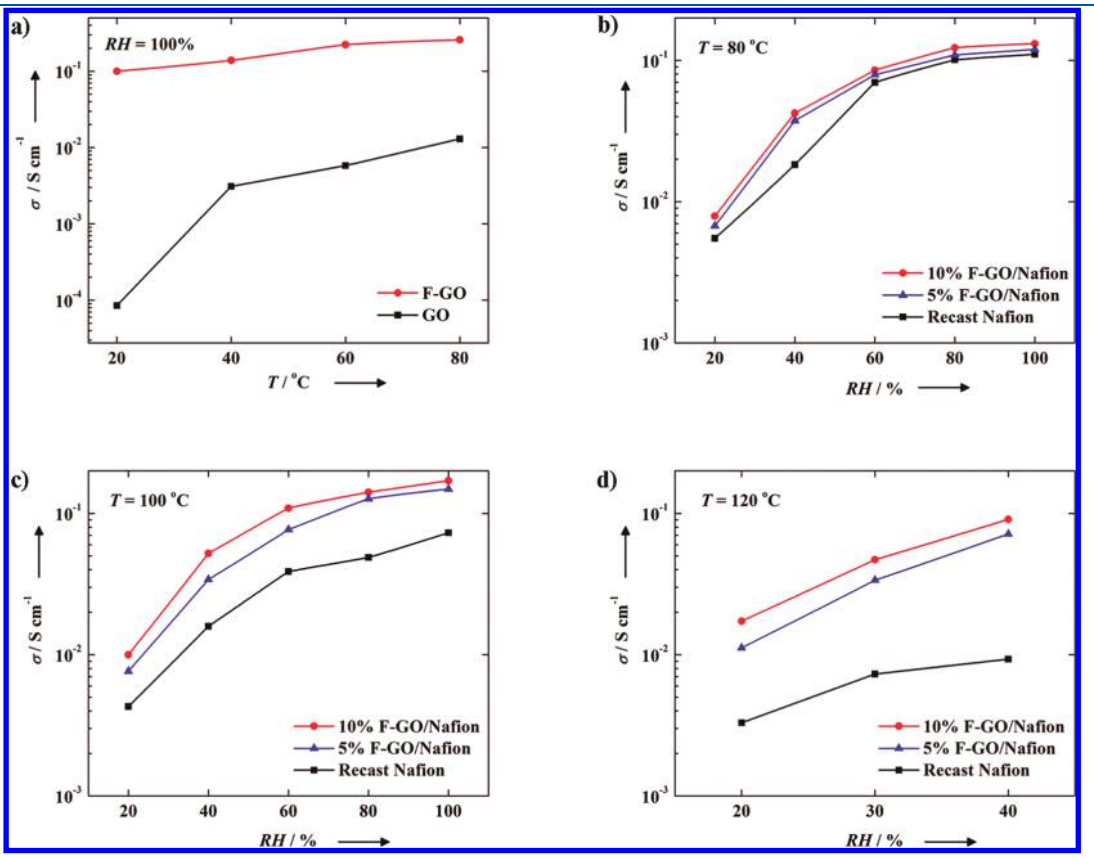

Figure 6. (a) Proton conductivity (σ) comparison between GO and F-GO powders. Proton conductivity of recast Nafion and F-GO composite membrane with doping levels of 5 and 10% at temperatures (T) of (b) 80 °C, (c) 100 °C, and (d) 120 °C at various relative humidities (RHs).

dx.doi.org/10.1021/jp204610j |J. Phys. Chem. C 2011, 115, 20774–20781

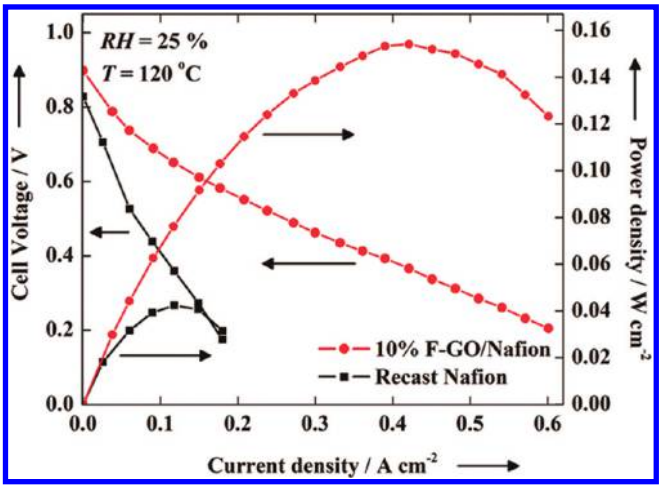

Figure 7. MEA polarization and power density curves for 10 wt % F-GO/Nafion and recast Nafion membranes, with commercial E-TEK 20 wt % Pt/C catalyst (anode 0.1 mg_{Pt} cm^{-2}, vathode 0.2 mg_{Pt} cm^{-2}) in a single-cell H_2/O_2 system at the temperature (T) of 120 °C and 25% relative humidity (RH).

matrix of Nafion has significantly increased the proton conductivity, particularly at the high temperature of 120 °C with low relative humidity. Figure 5b−d clearly reveals that increasing the F-GO nanofiller content can effectively enhance the proton conductivity of the Nafion nanocomposite membranes, as at 120 °C and 30% relative humidity the proton conductivity of 10 wt % F-GO/Nafion was 0.047 S cm^{-1}, an almost 4-fold improvement over 0.012 S cm^{-1} for the recast Nafion membrane. This can be explained based on the Grotthuss mechanism,[63] where protons diffuse through the hydrogen bond network of water molecules. Since F-GO has an extremely high surface area with an enormous amount of sulfonated functional groups, it holds more water and consequently could facilitate the transfer of more protons. The increase of F-GO nanofiller loading extends the number of available ion exchange sites per cluster, resulting in the increment of proton mobility in the membrane at high temperatures and low humidity values.

Figure 7 displays the polarization and power density curves for the 10 wt % F-GO/Nafion composite and recast Nafion in a single-cell H_2/O_2 MEA system operating at 120 °C and 25% relative humidity. The peak power density for 10 wt % F-GO/Nafion was 0.15 W cm^{-2}, approximately 3.6 times higher than that of recast Nafion (0.042 W cm^{-2}). At a cell voltage of 0.6 V, 10 wt % F-GO/Nafion showed a current density of 0.16 A cm^{-2}, about 3.5 times higher than recast Nafion (0.046 A cm^{-2}). These results are in direct agreement with the membrane proton conductivity analysis, as 10 wt % F-GO/Nafion displayed a substantial performance increase through MEA testing compared with recast Nafion under typical PEMFC conditions. Clearly, F-GO/Nafion nanocomposites offer significant promise as electrolyte membranes for PEMFC applications operating at elevated temperatures, owing to the beneficial structural and mechanical properties arising due to F-GO incorporation.

4. CONCLUSION

In summary, a sulfonic acid functionalized graphene oxide Nafion nanocomposite (F-GO/Nafion) has been presented as a potential proton exchange membrane replacement for low humidity and high temperature PEMFC applications. F-GO/Nafion nanocomposites demonstrated a significant proton conductivity improvement (4 times) over the unmodified one at a low humidity value of 30% and high temperature of 120 °C. Under similar operating conditions, single-cell MEA testing also revealed a significantly higher performance of 10 wt % F-GO/Nafion membrane than that of the recast Nafion, displaying peak power densities of 0.15 and 0.042 Wcm^{-2}, respectively. F-GO incorporation clearly offers substantial PEMFC performance improvements at elevated temperatures, and further investigations are underway to optimize these composite membranes and determine their chemical and mechanical stabilities.

AUTHOR INFORMATION

Corresponding Author

*E-mail: zhwchen@uwaterloo.ca. Telephone: 519-888-4567 Ext. 38664. Fax: 519-746-4979.

ACKNOWLEDGMENT

This work was financially supported by the Natural Sciences and Engineering Research Council of Canada (NSERC) and the University of Waterloo.

REFERENCES

(1) Vielstich, W.; Lamm, A.; Gasteiger, H. *Handbook of Fuel Cells: Advances in Electrocatalysis, Materials, Diagnostics and Durability*; Wiley: New York, 2003.
(2) Yamada, M.; Li, D.; Honma, I.; Zhou, H. *J. Am. Chem. Soc.* **2005**, *127*, 13092.
(3) Arico, A.; Baglio, V.; Di Blasi, A.; Creti, P. *Solid State Ionics* **2003**, *161*, 251.
(4) Di Noto, V.; Gliubizzi, R.; Negro, E.; Pace, G. *J. Phys. Chem. B* **2006**, *110*, 24972.
(5) Ladewig, B.; Knott, R.; Hill, A.; Riches, J.; White, J.; Martin, D.; da Costa, J.; Lu, G. *Chem. Mater.* **2007**, *19*, 2372.
(6) Li, Q.; He, R.; Jensen, J.; Bjerrum, N. *Chem. Mater.* **2003**, *15*, 4896.
(7) Licoccia, S.; Traversa, E. *J. Power Sources* **2006**, *159*, 12.
(8) Hickner, M.; Ghassemi, H.; Kim, Y.; Einsla, B.; McGrath, J. *Chem. Rev* **2004**, *104*, 4587.
(9) Bae, B.; Ha, H.; Kim, D. *J. Membr. Sci.* **2006**, *276*, 51.
(10) Chen, Z.; Holmberg, B.; Li, W.; Wang, X.; Deng, W.; Munoz, R.; Yan, Y. *Chem. Mater.* **2006**, *18*, 5669.
(11) Jalani, N.; Dunn, K.; Datta, R. *Electrochim. Acta* **2005**, *51*, 553.
(12) Kannan, R.; Kakade, B.; Pillai, V. *Angew. Chem., Int. Ed.* **2008**, *47*, 2653.
(13) Kumar, B.; Fellner, J. *J. Power Sources* **2003**, *123*, 132.
(14) Mauritz, K.; Moore, R. *Chem. Rev* **2004**, *104*, 4535.
(15) Tricoli, V.; Nannetti, F. *Electrochim. Acta* **2003**, *48*, 2625.
(16) Chalkovaa, E.; Wang, C.; Komarneni, S.; Lee, J.; Fedkin, M.; Lvov, S. *ECS Trans* **2009**, *25*, 1141–1150.
(17) Kalappa, P.; Lee, J. *Polym. Int.* **2007**, *56*, 371.
(18) Divigalpitiya, W.; Frindt, R.; Morrison, S. *Science* **1989**, *246*, 369.
(19) Kim, F.; Cote, L.; Huang, J. *Adv. Mater.* **1954**, 22.
(20) Yang, Q.; Liu, J.; Yang, J.; Kapoor, M.; Inagaki, S.; Li, C. *J. Catal.* **2004**, *228*, 265.
(21) Yang, S.; Feng, X.; Wang, L.; Tang, K.; Maier, J.; Müllen, K. *Angew. Chem., Int. Ed.* **2010**, *49*, 4795.
(22) Wilson, N.; Pandey, P.; Beanland, R.; Young, R.; Kinloch, I.; Gong, L.; Liu, Z.; Suenaga, K.; Rourke, J.; York, S. *ACS Nano* **2009**, *3*, 2547.

(23) Dikin, D.; Stankovich, S.; Zimney, E.; Piner, R.; Dommett, G.; Evmenenko, G.; Nguyen, S.; Ruoff, R. *Nature* **2007**, *448*, 457.
(24) Mkhoyan, K.; Contryman, A.; Silcox, J.; Stewart, D.; Eda, G.; Mattevi, C.; Miller, S.; Chhowalla, M. *Nano Lett.* **2009**, *9*, 1058.
(25) Yu, A.; Roes, I.; Davies, A.; Chen, Z. *Appl. Phys. Lett.* **2010**, *96*, 253105.
(26) Stankovich, S.; Dikin, D.; Dommett, G.; Kohlhaas, K.; Zimney, E.; Stach, E.; Piner, R.; Nguyen, S.; Ruoff, R. *Nature* **2006**, *442*, 282.
(27) Stankovich, S.; Piner, R.; Chen, X.; Wu, N.; Nguyen, S.; Ruoff, R. *J. Mater. Chem.* **2006**, *16*, 155.
(28) Gnana Kumar, G.; Kim, A.; Suk Nahm, K.; Elizabeth, R. *Int. J. Hydrogen Energy* **2009**, *34*, 9788.
(29) Hummers, W., Jr; Offeman, R. *J. Am. Chem. Soc.* **1958**, *80*, 1339.
(30) Lerf, A.; He, H.; Forster, M.; Klinowski, J. *J. Phys. Chem. B* **1998**, *102*, 4477.
(31) Wang, Y.; Yang, D.; Zheng, X.; Jiang, Z.; Li, J. *J. Power Sources* **2008**, *183*, 454.
(32) Nagarale, R.; Shin, W.; Singh, P. *Polym. Chem.* **2009**, *1*, 388.
(33) Uchida, H.; Ueno, Y.; Hagihara, H.; Watanabe, M. *J. Electrochem. Soc.* **2003**, *150*, A57.
(34) Wilson, M.; Valerio, J.; Gottesfeld, S. *Electrochim. Acta* **1995**, *40*, 355.
(35) Holmberg, B.; Yan, Y. *J. Electrochem. Soc.* **2006**, *153*, A146.
(36) Wu, Z.; Sun, G.; Jin, W.; Hou, H.; Wang, S.; Xin, Q. *J. Membr. Sci.* **2008**, *313*, 336.
(37) Lee, C.; Park, H.; Lee, Y.; Lee, R. *Ind. Eng. Chem. Res.* **2005**, *44*, 7617.
(38) Mikhailenko, S.; Guiver, M.; Kaliaguine, S. *Solid State Ionics* **2008**, *179*, 619.
(39) Sone, Y.; Ekdunge, P.; Simonsson, D. *J. Electrochem. Soc.* **1996**, *143*, 1254.
(40) Hensley, J.; Way, J. *J. Power Sources* **2007**, *172*, 57.
(41) Majsztrik, P.; Satterfield, M.; Bocarsly, A.; Benziger, J. *J. Membr. Sci.* **2007**, *301*, 93.
(42) D'Epifanio, A.; Navarra, M.; Weise, F.; Mecheri, B.; Farrington, J.; Licoccia, S.; Greenbaum, S. *Chem. Mater.* **2009**, *22*, 813.
(43) Tian, L.; Meziani, M.; Lu, F.; Kong, C.; Cao, L.; Thorne, T.; Sun, Y. *ACS Appl. Mater. Interface* **2010**, 183.
(44) Wang, H.; Hao, Q.; Yang, X.; Lu, L.; Wang, X. *ACS Appl. Mat. Interface* **2010**, *2*, 821.
(45) Whitby, R.; Korobeinyk, A.; Glevatska, K. *Carbon* **2010**, *49*, 722.
(46) Xu, L.; Yang, W.; Neoh, K.; Kang, E.; Fu, G. *Macromolecules* 2010, *197*.
(47) Haubner, K.; Murawski, J.; Olk, P.; Eng, L.; Ziegler, C.; Adolphi, B.; Jaehne, E. *ChemPhysChem* **2010**, *11*, 2131.
(48) Park, S.; Dikin, D.; Nguyen, S.; Ruoff, R. *J. Phys. Chem. C* **2009**, *113*, 15801.
(49) Wang, G.; Wang, B.; Park, J.; Yang, J.; Shen, X.; Yao, J. *Carbon* **2009**, *47*, 68.
(50) Okpalugo, T.; Papakonstantinou, P.; Murphy, H.; McLaughlin, J.; Brown, N. *Carbon* **2005**, *43*, 153.
(51) Lian, Y.; Liu, Y.; Jiang, T.; Shu, J.; Lian, H.; Cao, M. *J. Phys. Chem. C* **2010**, *114*, 9659.
(52) Chu, D.; Gervasio, D.; Razaq, M.; Yeager, E. *J. Appl. Electrochem.* **1990**, *20*, 157.
(53) Laporta, M.; Pegoraro, M.; Zanderighi, L. *Phys. Chem. Chem. Phys.* **1999**, *1*, 4619.
(54) Lavorgna, M.; Mascia, L.; Mensitieri, G.; Gilbert, M.; Scherillo, G.; Palomba, B. *J. Membr. Sci.* **2007**, *294*, 159.
(55) Ostrowska, J.; Narebska, A. *Colloid Polym. Sci.* **1983**, *261*, 93.
(56) Rieke, P.; Vanderborgh, N. *J. Membr. Sci.* **1987**, *32*, 313.
(57) Hamwi, A.; Marchand, V. *J. Phys. Chem. Solids* **1996**, *57*, 867.
(58) Mermoux, M.; Chabre, Y.; Rousseau, A. *Carbon* **1991**, *29*, 469.
(59) Leuchs, M.; Zundel, G. *J. Chem. Soc., Faraday Trans. 2* **1978**, *74*, 2256.
(60) Liang, Z.; Chen, W.; Liu, J.; Wang, S.; Zhou, Z.; Li, W.; Sun, G.; Xin, Q. *J. Membr. Sci.* **2004**, *233*, 39.
(61) Wool, R. *J. Polym. Sci., Polym. Phys.* **1975**, *13*, 1795.
(62) Si, Y.; Samulski, E. *Nano Lett.* **2008**, *8*, 1679.
(63) Agmon, N. *Chem. Phys. Lett.* **1995**, *244*, 456.